

Performance of FRP confined and unconfined geopolymer concrete exposed to sulfate attacks

Radhwan Alzebaree^{*2,4}, Mehmet Eren Gülşan^{1a}, Anil Niş^{3b},
Alaa Mohammedameen^{2,4c} and Abdulkadir Çevik^{1d}

¹ Department of Civil Engineering, Gaziantep University, Gaziantep, Turkey

² Department of Civil Engineering, Duhok Polytechnic University, Duhok, Iraq

³ Department of Civil Engineering, İstanbul Gelisim University, İstanbul, Turkey

⁴ Department of Civil Engineering, Newroz University, Duhok, Iraq

(Received April 16, 2018, Revised August 7 2018, Accepted August 18, 2018)

Abstract. In this study, the effects of magnesium sulfate on the mechanical performance and the durability of confined and unconfined geopolymer concrete (GPC) specimens were investigated. The carbon and basalt fiber reinforced polymer (FRP) fabrics with 1-layer and 3-layers were used to evaluate the performances of the specimens under static and cyclic loading in the ambient and magnesium sulfate environments. In addition, the use of FRP materials as a rehabilitation technique was also studied. For the geopolymerization process of GPC specimens, the alkaline activator has selected a mixture of sodium silicate solution (Na_2SiO_3) and sodium hydroxide solution (NaOH) with a ratio ($\text{Na}_2\text{SiO}_3/\text{NaOH}$) of 2.5. In addition to GPC specimens, an ordinary concrete (NC) specimens were also produced as a reference specimens and some of the GPC and NC specimens were immersed in 5% magnesium sulfate solutions. The mechanical performance and the durability of the specimens were evaluated by visual appearance, weight change, static and cyclic loading, and failure modes of the specimens under magnesium sulfate and ambient environments. In addition, the microscopic changes of the specimens due to sulfate attack were also assessed by scanning electron microscopy (SEM) to understand the macroscale behavior of the specimens. Results indicated that geopolymer specimens produced with nano-silica and fly ash showed superior performance than the NC specimens in the sulfate environment. In addition, confined specimens with FRP fabrics significantly improved the compressive strength, ductility and durability resistance of the specimens and the improvement was found higher with the increased number of FRP layers. Specimens wrapped with carbon FRP fabrics showed better mechanical performance and durability properties than the specimens wrapped with basalt FRP fabrics. Both FRP materials can be used as a rehabilitation material in the sulfate environment.

Keywords: Geopolymer Concrete (GPC); Fiber Reinforced Polymer (FRP); static and cyclic loading; magnesium sulfate environment; nano-silica

1. Introduction

The durability of the structures subjected to chemical attacks is a significant issue due to the increased number of hazardous wastes to the environment. The structural elements should have adequate durability properties as well as adequate resistance to the external structural loads to resist the degradation effects of the chemical environments. For this purpose, studies continue to prevent or decrease the harmful effects of the chemical environment to the overall structural system. In addition to this, during the cement manufacturing process, a considerable amount of CO_2 is released to the environment, which is a significant trouble

for both cement producers and human being. Therefore, studies are focused on the novel types of concrete to prevent the hazardous effect of OPC production to the environment. Recently, a new type of environmentally-friendly geo-polymer concrete becomes popular and it gives a chance to replace cement by appropriate aluminosilicate source such as fly ash (Nazari and Sanjayan 2015). The geopolymer concrete (GPC) has considerable advantages over OPC concrete in terms of both environmental (Deb *et al.* 2014, Duxson *et al.* 2007, Khale and Chaudhary 2007, Partha *et al.* 2013), and mechanical performance and durability properties like high early strength, high flexural strength good resistance against sulfate and acid attacks, low creep and low shrinkage (Davidovits 1994, Hardjito *et al.* 2004, Nazari and Sanjayan 2015, Wallah *et al.* 2005).

The brittleness nature of the geopolymer concrete remains a critical issue as in the case of OPC concrete. Recently, fiber reinforced polymer (FRP) composites have been used as a method of confinement to prevent the brittle failure and to improve the mechanical properties of the concrete structures (Bakis *et al.* 2002). One of the most common rehabilitation techniques for the circular columns

*Corresponding author, Ph.D. Student,

E-mail: alzebaree@gmail.com

^a Assistant Professor, Ph.D., E-mail: gulsan@gantep.edu.tr

^b Ph.D., E-mail: anis@gelisim.edu.tr

^c Ph.D. Student, E-mail: amalatroschi@gmail.com

^d Professor, E-mail: akcevik@gantep.edu.tr

is the FRP wrapping (Abdelrahman and El-Hacha 2011). The confined stress of FRP wrapping can be higher than the confining stress of conventional steel reinforcement in concrete structural elements due to the high strength and ductility of FRP (Lokuge *et al.* 2010). In addition, FRP wrappings are preferred for the repair and strengthening of structural elements due to the advantages of lightweight, low thermal conductivity, and high resistance to corrosion and chemical attacks (Nanni and Bradford 1995, Garg *et al.* 2017, Hamilton *et al.* 2009, Gülşan *et al.* 2018). Therefore, FRP wrappings are used as a confinement method for the geopolymer concrete specimens.

Researchers mostly deal with the production processes of the geopolymer concrete and the effects of manufacturing limitations on the physical and mechanical properties of geopolymer concrete. Due to the limited studies about the durability of geopolymer concretes, the use of geopolymer concretes in structural elements remains limited (Mobili *et al.* 2016). Sulfate attack is one of the hazardous environments to the durability of the concrete structural elements. Structural elements such as foundations are exposed to sulfate environment (groundwater, soil, and seawater). For this reason, the performance of structural elements under sulfate environment is a significant durability issue for the life safety of the structures (Taylor *et al.* 2001, Tulliani *et al.* 2002).

Due to the very few studies investigating the durability of GPC specimens under sulfate attack, this study investigated the effect of sulfate environment on the GPC concrete. Static and cyclic loadings were applied on the geopolymer concrete specimens to simulate the mechanical performance of the concrete under chemical environment. One of the aims of the study is to investigate the reinforcing effect of different FRP wrappings with different layers to reduce the harmful effects of magnesium sulfate attacks. In addition, the use of FRP wrappings as a rehabilitation technique was also studied. The microscale changes of the specimens were also assessed using SEM analysis to understand the macroscale behavior. The obtained outcomes

of the study can be important for structures exposed to sulfate attack, and they can be used to improve the service life of structures.

2. Experimental program

2.1 Materials and mix design

Geopolymer concrete (GPC) and OPC concrete reinforced with different layers of carbon and basalt FRP fibers were used in the research to evaluate the performances of the concrete under 5% magnesium sulfate attack. F-type fly ash was obtained from Ceyhan Sugözü thermal power plant and nano silica was ordered from Norway was used as a partial replacement to improve the chemical resistance of the GPC (Lloyd and Rangan 2010). The crushed limestone was used as coarse and fine aggregates with specific gravities of 2.68 and 2.62, respectively. The aggregate grading curves were found similar to earlier studies (Hardjito and Rangan 2005, Wallah *et al.* 2005). A high range water reducing admixture was used as a superplasticizer for workability. The physical and chemical properties of FA, OPC and NS were summarized in Table 1.

The alkaline solution of GPC was prepared with a mixture of sodium silicate solution (Na_2SiO_3) and sodium hydroxide solution (NaOH). The sodium silicate solution (Na_2O :13.7%, SiO_2 : 29.4, water: 55.9% by mass) was obtained from a local supplier. The sodium hydroxide (NaOH) solution was obtained in pellets with 97%-98% purity. The NaOH solids were dissolved in water with 14M concentration, which was considered to be weakest concentration amount of GPC under chemical attack (Kumaravel and Girija 2013). The alkaline solution was prepared in the laboratory at least one day prior to its use. NaOH/ Na_2SiO_3 ratio varies in the range of 1.5 to 2.5 for economic reasons (Olivia and Nikraz 2012) and it was used as 2.5 in this study. An activator liquid to fly ash ratio was

Table 1 Chemical composition and physical properties of FA, NS and OPC

Materials	CaO	SiO ₂	Al ₂ O ₃	Fe ₂ O ₃	MgO	SO ₃	K ₂ O	Na ₂ O	Loss of ignition	Specific gravity	Blain fineness (m ² /kg)
FA (%)	2.24	59.20	24.40	7.07	1.40	0.29	3.40	0.38	1.52	2.30	379
NS (%)	-	99.80	-	-	-	-	-	-	<1.00	2.20	-
OPC (%)	62.11	19.10	5.20	2.90	1.17	2.63	3.88	0.17	2.99	3.15	326

Table 2 Mix design of GPC and NC mixtures (kg/m³)

Mix	FA	Cement	Na ₂ SiO ₃ + NaOH	Water	Fine Agg.	Coarse Agg.	NS	SP	Na ₂ SiO ₃ / NaOH	Alkali/binder	W/C
GPC	485	-	225	-	549.5	1098.8	15	7.5	2.5	0.45	-
NC	-	476	-	214.2	562.6	1125	-	2.38	-	-	0.45

Table 3 The properties of fabric sheets

FRP types	Tensile strength (MPa)	Modulus of elasticity (GPa)	Elongation (%)	Thickness (mm)	Area weight (g/m ²)
BFRP	2100	105	2.6	0.3	300
CFRP	4900	240	2	0.3	300

Table 4 The properties of the epoxy

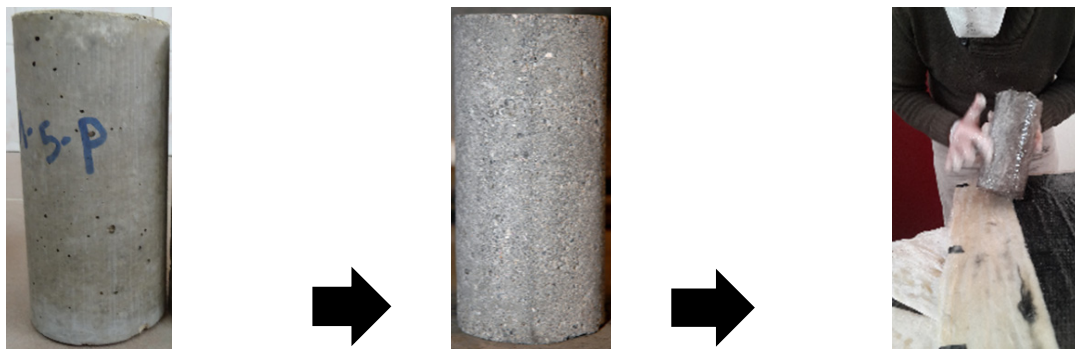
FRP types	Pot life at 20°C (Min)	Flexural strength 7 days (N/mm ²)	Compressive strength 7 days (N/mm ²)	Bond strength 7 days (N/mm ²)	Modulus of elasticity 7 days (GPa)
Teknobond 300 Tix	30	≥ 25	≥62.5	≥3	>20

selected as 0.45. Mix design of the GPC and NC were given in Table 2.

In the study, confinement of cylinder specimens of 100 mm in diameter and 200 mm in length was provided by using uni-directional carbon fiber reinforced polymer (CF) and basalt fiber reinforced polymer (BF) fabrics to investigate the effect of magnesium sulfate attack on the durability and mechanical performance of concretes. The properties of the FRP materials were presented in Table 3. The epoxy adhesive, Teknobond 300 Tix, was used and its general properties were given in Table 4.

2.2 Casting and curing of specimens

Mixing procedure was as following; coarse aggregates (SSD condition) and fine aggregates, fly ash, cement (for related mixes) were added into the mixer and mixed for 3 minutes. The prepared alkaline solution and superplasticizer added in 1 minute and further mixed for 3 minutes for homogeneity (Jo *et al.* 2007). After casting, specimens were covered using vacuum bagging film to prevent evaporation of the alkaline solution and kept for 24 hrs at room temperature. Then, GPC specimens were cured together



(a) Concrete surface preparation



(b) Preparation of sheets



(c) Application and impregnation of the FRP fabric

Fig. 1 Main steps (a, b and c) of applying FRP fabric

with molds in an oven at 70°C for 48 hrs to activate geopolymerization since strength enhancement was found insignificant beyond 48 hrs (Hardjito *et al.* 2004). After oven temperature at 23±2°C in the laboratory for 28 days. For the OPC concrete, specimens were cured in a water tank for 28 days.

2.3 Specimen preparation and testing

After curing procedure, some of the cylinder specimens were wrapped by carbon and basalt FRP fabrics according to the given FRP application procedure on the specimen

surfaces. FRP wrapping procedure was completed in three steps; preparation the concrete surface (a), preparation of FRP sheets (b) and impregnation and application of the FRP fabrics on the concrete outer surface (c) as shown in Fig. 1.

In the first stage, wire brush was used to eliminate the loosely held powders that remained on the concrete surface and air compressor was also utilized to clean the surfaces. In the second stage, the FRP sheets were cut to get FRP sheets with lengths of 115 cm for three-layer FRP wrapping and 48 cm for one-layer FRP wrapping. For the outer layer of FRP wrappings, specimens were covered by the fabric sheets with an overlapping length of 15 cm to get a strong

Table 5 Details of test specimens

Test series	Type of concrete	No. of samples	Confined				Control sample	Sulfate exposed	Wrapping age		Testing age		Specimen ID	
			Unconfined	BFRP		CFRP			28-days	90-days	28-days	90-days		
				1-layer	3-layers	1-layer								3-layers
A		3	✓				✓			✓		UGC-28		
		3		✓			✓		✓		✓	BF1GC-28		
		3			✓		✓		✓		✓	BF3GC-28		
		3				✓	✓		✓		✓	CF1GC-28		
		3				✓	✓		✓		✓	CF3GC-28		
B		6a	✓								✓	UGC-90		
		6a		✓			✓				✓	BF1GC-90		
		3			✓		✓				✓	BF3GC-90		
		6a				✓	✓				✓	CF1GC-90		
		3				✓	✓				✓	CF3GC-90		
C	GPC	3		✓					✓		✓	BF1GC-A		
		3			✓		✓		✓		✓	BF3GC-A		
		3				✓	✓		✓		✓	CF1GC-A		
		3				✓	✓		✓		✓	CF3GC-A		
D		6a	✓				✓				✓	UGS-90		
		6a		✓			✓	✓			✓	BF1GS-90		
		3			✓		✓	✓			✓	BF3GS-90		
		6a				✓	✓	✓			✓	CF1GS-90		
		3				✓	✓	✓			✓	CF3S-90		
E		3		✓			✓		✓		✓	BF1GS-A		
		3			✓		✓		✓		✓	BF3GS-A		
		3				✓	✓		✓		✓	CF1GS-A		
		3				✓	✓		✓		✓	CF3GS-A		
F	NC	3	✓								✓	UNC-90		
		3		✓			✓				✓	BF1NC-90		
		3			✓		✓				✓	CF1NC-90		
G		3	✓				✓				✓	UNS-90		
		3		✓			✓	✓			✓	BF1NS-90		
		3			✓		✓	✓			✓	CF1NS-90		

bond between the layers and prevent FRP slippage. In the last stage, implementation of FRP fabrics on concrete surfaces was realized by three operations: (a) coating inner sides of the FRP fabrics with epoxy resin; (b) FRP installation was applied on the concrete surfaces; and (c) each layer of the FRP fabrics was impregnated by epoxy resins to obtain perfect bond between concrete surface and FRP sheets. The used epoxy resin was prepared using a hardener and a resin with a ratio of 1:3 by mass. The epoxy resin was also used on concrete surfaces to fill the pores of the concrete surface before covering the specimens with FRP fabrics as shown in Fig. 1. In addition, the fibers orientation of FRP fabrics was taken into consideration during the covering process to ensure alignment of fibers perpendicular to the axial direction of loading. After FRP installation, specimens were left at room temperature for 7 days to obtain the required strength of the epoxy resins (Baldvin 2011).

2.4 Specimens for mechanical tests

As a result of the FRP installation procedure, unconfined specimens (without wrapping), specimens wrapped by carbon FRP with 1 layer and 3 layers and specimens wrapped by basalt FRP with 1 layer and 3 layers were obtained. In addition, F-type fly ash based geopolymer concrete including nano-silica and OPC concrete were produced and the specimens were exposed to both magnesium sulfate environment and ambient environment (laboratory condition). Geopolymer specimens (unexposed specimens) were tested at the ages of 28 days and 90 days, while OPC concrete specimens (unexposed specimens) were tested at only 90 days under ambient environment. Both geopolymer and OPC specimens exposed to the magnesium sulfate environment were tested at the age of 90 days (28 days curing regime and the remaining days under magnesium sulfate environment). The produced and tested specimens were summarized in details as shown in Table 5.

Series A: 15 GPC samples under control condition (3 unwrapped and 12 wrapped) were tested at 28 days and the confinement is applied at the end of 28 days.

Series B: 24 GPC samples under control condition (6 unwrapped and 18 wrapped) were tested at 90 days and the confinement is applied at the end of 28 days.

Series C: 12 wrapped GPC samples under control condition were tested at 90 days and the confinement is applied at the end of 90 days.

Series D: 24 GPC samples exposed to 5% sulfate environment (6 unconfined and 18 confined) were tested at 90 days. Some of the samples were confined by FRP fabrics at 28 days and then subjected to 8 weeks of sulfate solution. The sulfate exposed samples were tested at 90 days.

Series E: 12 unwrapped GPC samples subjected to 5% sulfate environment for duration of two months. Then, the confinement is applied on the sulfate affected specimens and tested at the age of 90 days to evaluate the effect of FRP wrapping as a means of rehabilitation.

Series F: 9 NC samples under control condition (3 unwrapped and 6 wrapped) were tested at 90 days and the confinement is applied at the age of 28 days.

Series G: 9 NC samples under 5% sulfate solution (3 unwrapped and 6 wrapped) were tested at 90 days after 8 weeks of exposure to the sulfate solution. The FRP confinement is applied at the age of 28 days. In a total, 105 specimens were prepared and tested in this study.

2.5 Specimen nomenclature

In the test procedure, there were 29 different cases and specimens were coded accordingly. The first term indicated the fabric types with the number of layers; CF1, BF1 and CF3, BF3 showed the specimens wrapped by carbon and basalt fabrics with 1 and 3 layers, and U showed the unconfined (unwrapped) specimens. The second term (types of concrete); G and N indicated the geopolymer concrete and normal (OPC) concrete, respectively. The third term (types of the environment); C and S indicated control environment (ambient or lab condition) and magnesium sulfate environment, respectively. The last terms (-28, -90, -A) indicated the test days of the specimens. The term of -28 indicated that specimens were tested at the age of 28 days at the end of curing. The term of -90 implied that specimens were tested at the age of 90 days. In the first 28 days, specimens were cured, then FPR wrappings were realized and the specimens were exposed to chemical solutions for the remaining days. The term of -A identified that specimens were first cured and the remaining days specimens were exposed to chemical solution up to 90 days. Then FRP wrappings were realized and specimens were tested. For instance, UGC-90 and UGS-90 referred to unconfined (U) geopolymer concrete (G) specimens under control (C) and magnesium sulfate environment (S) and tested at the age of 90 days, respectively. CF1GC-90 and CF1GC-A indicated specimens confined by carbon fiber with 1 layers (CF1) of geopolymer concrete (G) exposed to control environment (C) and tested at the age of 90 days (-90: FRP wrappings applied at 28.day and specimens were tested at 90.day) and at the age of 90 days (-A: FRP wrapping realized at the age of 90 days and immediately after specimens were tested).

2.6 Specimens under magnesium sulfate attack

There is no specific test method to assess the durability of concretes under chemical attack. ASTM C 267 test method (ASTM C267 2003) suggests that specimens should be immersed in water for 24 hours to obtain water saturated saturated specimens prior to chemical attacks. Therefore, specimens were soaked in water for 24 hours and initial saturated weights of the specimens were recorded. Then specimens were kept in 5% magnesium sulfate solution for a period of two months.

Simultaneously, control specimens were left in an ambient condition at a room temperature of $23 \pm 2^\circ\text{C}$ in the laboratory for two months for comparison. The specimens were removed from magnesium sulfate solution and residual chemical reaction products on the concrete surface were cleaned at the end of each week. Then specimens were left to drying under laboratory conditions at a temperature of $23 \pm 2^\circ\text{C}$ for 2 hours prior to weight measurements of the

specimens. The amount of deterioration due to magnesium sulfate attack was evaluated by visual inspection, weight change and compressive strength change of the specimens.

2.7 Test procedure

Compressive strength tests were realized on cylinder specimens with a diameter of 100 mm and length of 200 mm under static and cyclic loadings. Compressive strength tests were carried out using ASTM C39 standard (ASTM C39 2012). All compressive strength tests were conducted under displacement control with a rate of 0.2 mm/min. Two linear variable displacement transducers (LVDTs) were fixed to measure axial deformations in the specimens as shown in Fig. 2. Stress and strain data were obtained for each specimen using LVDT.

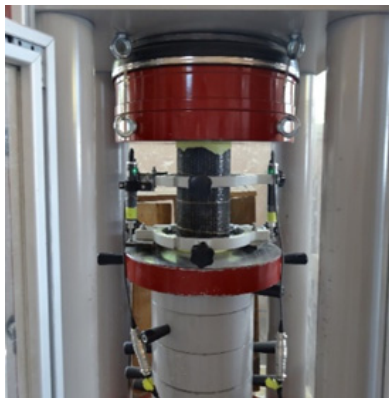


Fig. 2 Specimen under axial load

3. Experimental results and discussion

3.1 Visual inspection

Figs. 3 and 4 illustrate the visual appearances of the geopolymer and ordinary concrete specimens under 5% magnesium sulfate environment. Specimens maintained their initial conditions and there is no gypsum formation, color change, spalling or cracking were observed on the outermost surface of the specimens under sulfate environment, except for the very thin layer of efflorescence on the outermost surface of the specimens. All specimens remained structurally intact. Similar results were also reported by other researchers (Bakharev 2005, Visitanupong 2009). In addition, the outermost layers of carbon and basalt FRP fabrics remained unaffected after two months of exposure to sulfate environment. However, after cutting off the FRP fabrics for visual observation, both FRP fabrics was slightly influenced by the magnesium sulfate environment and the color change was observed to be highest for basalt FRP fabrics than the carbon FRP fabrics.

3.2 Weight change

Fig. 5 presents the weight change of the specimens under the ambient and 5% magnesium sulfate environments after the two months of chemical exposure. The decrease in the weight was observed for all specimens at ambient environment due to continuous hydration (Li and Roy 1988, Li and Ding 2003, Gülşan *et al.* 2018). The weight loss of OPC concrete was more than 3-times the weight loss

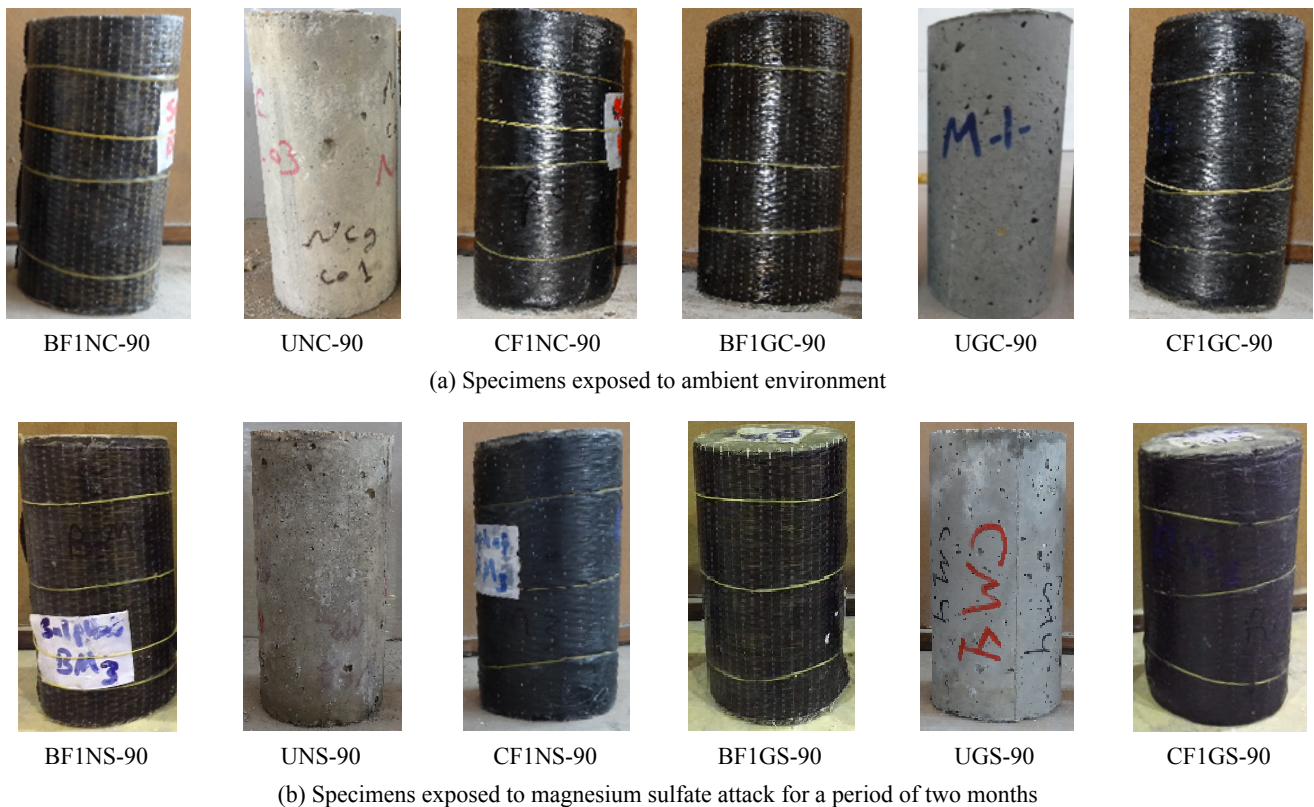


Fig. 3 Deterioration of specimens under magnesium sulfate and control environments

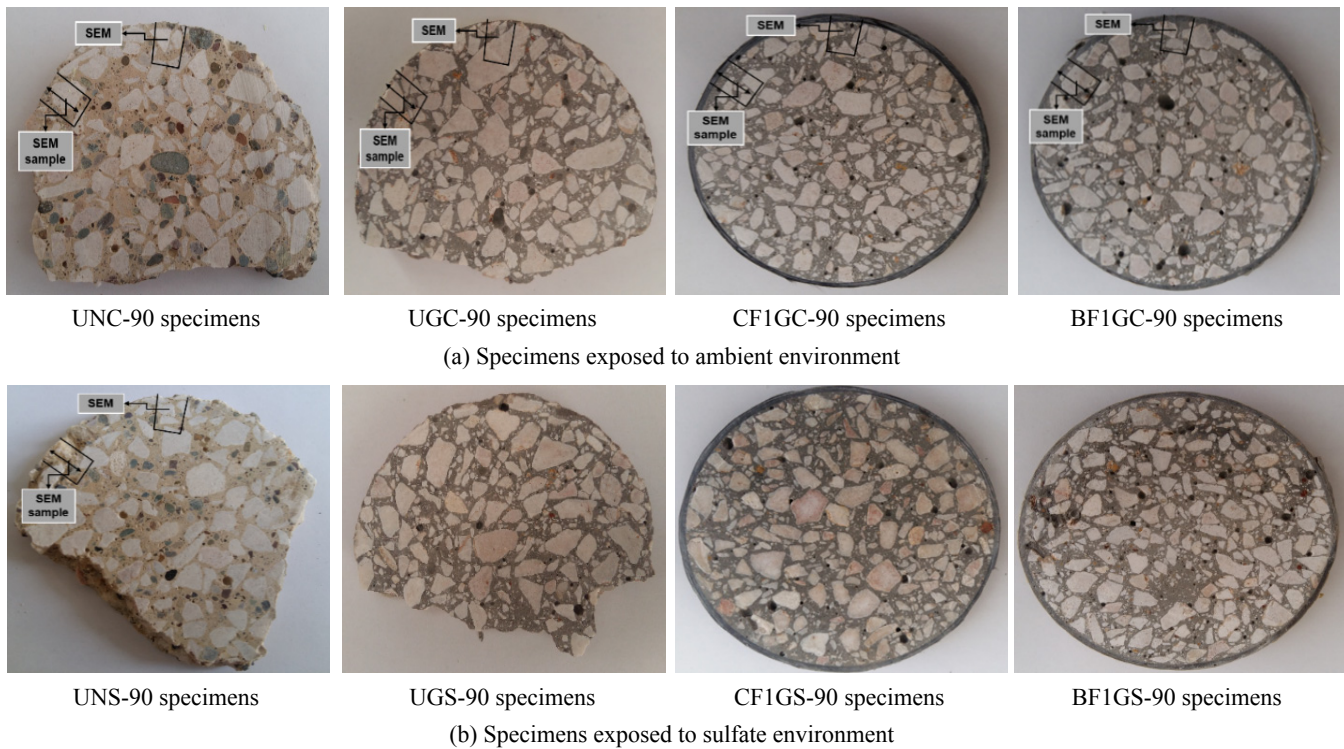


Fig. 4 Visual inspection of specimens under ambient condition and sulfate environment

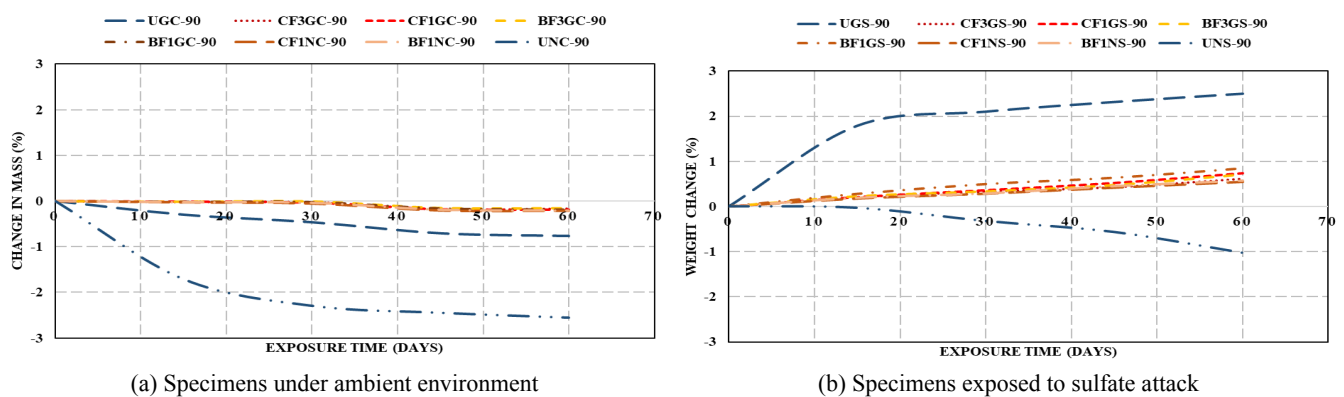


Fig. 5 Weight change of the specimens under ambient and magnesium sulfate environment

of GPC specimens as shown in Fig. 5(a). It can be attributed to the curing condition (70°C for 48 hours) of the GPC specimens since most of the hydration reactions took place on the first days. The similar weight losses were obtained for all specimens that wrapped with different layers of FRP fabrics. The 3 layers of FRP wrappings had no or negligible effect on weight change results in an ambient environment.

The weight gain was observed for all specimens under magnesium sulfate environment, except for the unconfined ordinary concrete (UNS-90 specimens). The highest weight gain was observed on unwrapped GPC specimens ($\sim 2.5\%$).

It may be attributed to the higher porosity of unwrapped GPC specimens resulted from the heat curing of the specimens. In addition, FRP wrappings decreased the amount of weight gain due to sulfate attack. The specimens with 3-layer FRP wrappings showed higher weight gain resistance than the specimens with 1-layer FRP wrapping.

The type of the FRP wrappings also affected the weight change results. The specimens wrapped with basalt FRP fabrics showed slightly increase in weight higher than the carbon FRP fabrics. The weight gain due to absorption of magnesium sulfate solution was also reported in the previous studies (Thokchom *et al.* 2010, Wallah and Rangan 2006). It may be attributed to an increase in volume by a factor of about two (Soroka 1979) and reduced density of concrete due to the formation of gypsum and ettringite resulted from the reactions between the chemical solution and cement. Therefore, the initial weight gains of the specimens may result from the lower reduction amount in relative density than the increase in relative volume (Attigbo and Rizkalla 1988). On the contrary, the weight loss ($\sim 1\%$) was observed on the unwrapped ordinary concrete specimens.

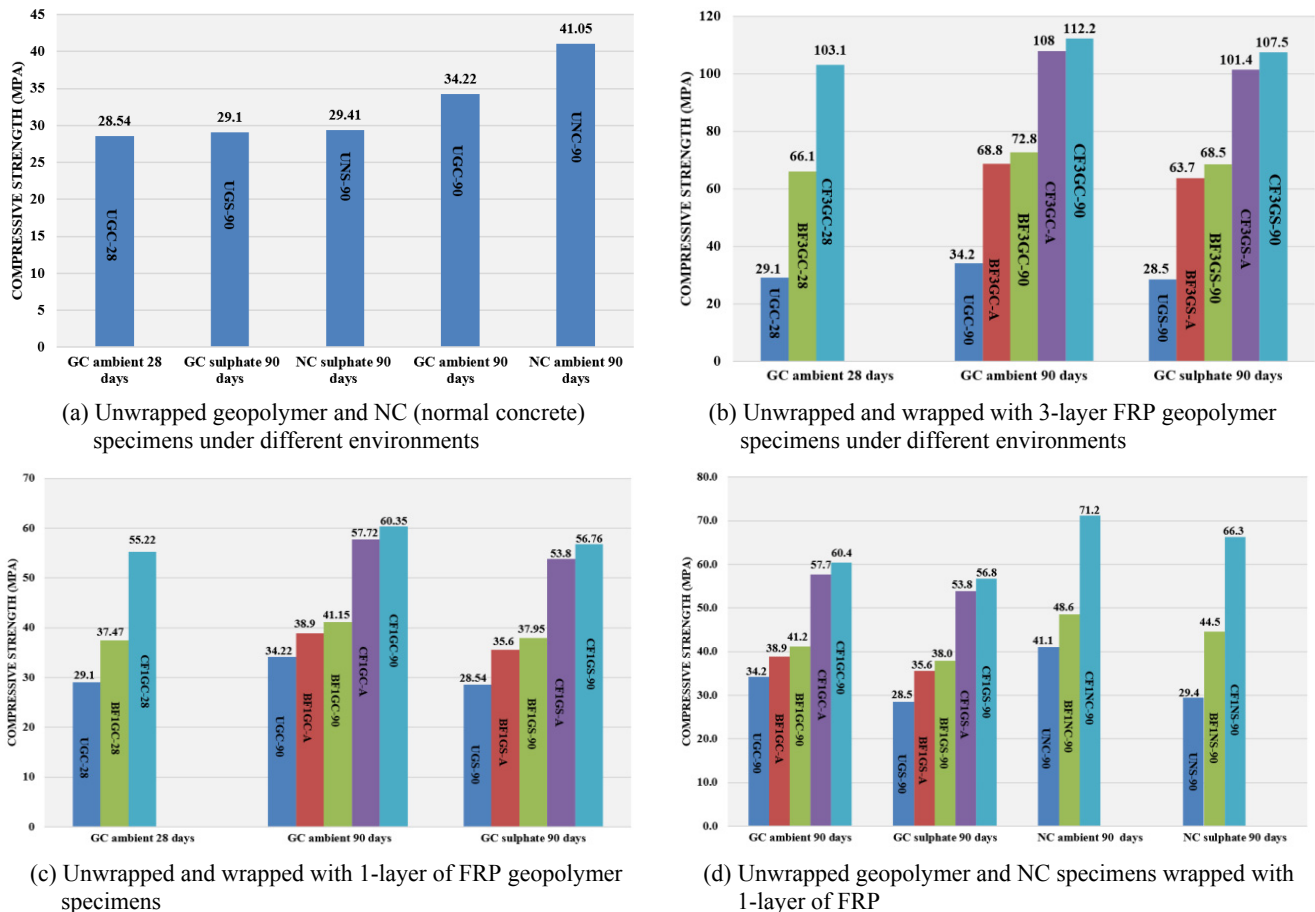


Fig. 6 Compressive strength of the specimens under different environment

3.2 Compressive strength and stress-strain behavior of the specimens

Fig. 6 presents the compressive strength of geopolymer and ordinary concrete specimens under ambient and magnesium sulfate environments. In general, specimens under ambient environment showed higher compressive strength results than the specimens under the sulfate environment. In addition, specimens with FRP wrappings showed significant enhancement in the compressive strength results and the compressive strength increased with an increase in the number of FRP layers. The highest and the lowest compressive strengths were obtained on the specimens wrapped with 3-layer of carbon FRP and 1-layer of basalt FRP, respectively. The magnesium sulfate environment reduced the compressive strength of the specimens, as expected.

3.2.1 Compressive strength of unwrapped specimens

Fig. 7 illustrates the stress-strain behavior of unwrapped specimens under the ambient and magnesium sulfate environments. The compressive strength of UGC-90 specimens showed 17.6% strength increase than the UGC-28 specimens. It can be attributed to the continuous hydration of the pozzolanic reaction of fly ash. Similar investigations reported in the previous studies (Liu *et al.* 2017, Çevik *et al.* 2018, Zhang and Zhang 2017).

UGS-90 specimens showed 16.6% and 1.92% compressive strength reduction as compared to compressive strengths of UGC-90 and UGC-28 specimens, respectively. The decline in compressive strength due to chemical attacks can be attributed to the weakest concentration amount of 14M NaOH solid in the production of geopolymer specimens (Kumaravel and Girija 2013). The reduction in the compressive strength of GPC specimens exposed to chemical attack may be attributed to destroy of the oxy-aluminum bridge (-Al-Si-O) of geopolymeric gel (Chindaprasirt *et al.* 2012). The similar trend was also observed for ordinary concrete specimens. The UNS-90 specimens showed 28.3% compressive strength reduction as compared to UNC-90 specimens. The GPC specimens showed lower compressive strength and strain values than the ordinary concrete specimens. It may be attributed to the low activity of fly ash (Chi and Huang 2013, Çevik *et al.* 2018) and low calcium content (Belkowitz *et al.* 2015, Dombrowski *et al.* 2007) for GPC specimens since the low calcium content in the fly ash did not participate in the calcium silicate hydrate formation (the main product that responsible for strength) (Chi and Huang 2013). In addition, another reason of the low compressive strength for GPC specimens may be due to the unreacted nano-silica particles in GPC since unreacted nano-silica particles can cause an excessive self-dehydration and cracks in the matrix that eventually reduces the compressive strengths of the geopolymer specimens (Belkowitz *et al.* 2015).

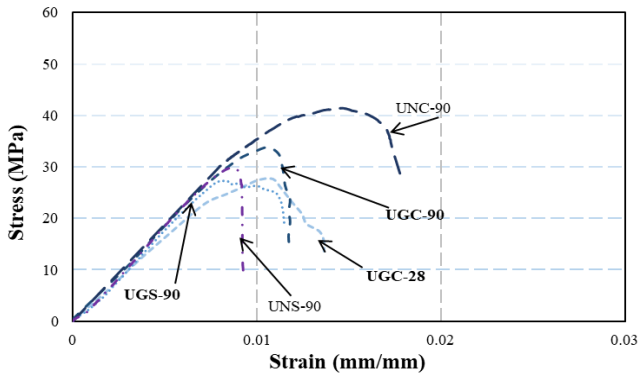


Fig. 7 Stress-strain behavior of unwrapped test specimens

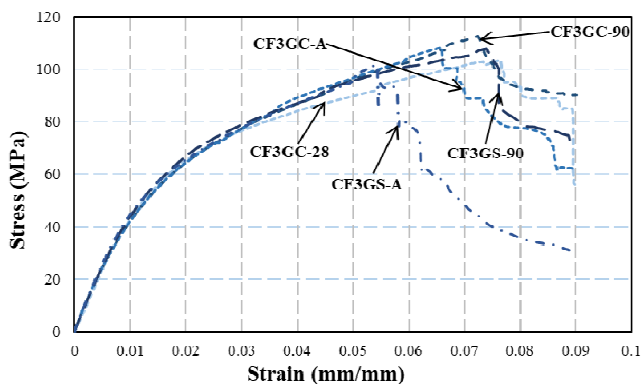
Degradation mechanism for sulfate attacks can be explained that sulfate ions diffuse into the hydrated cement paste and react with C3A in the presence of $\text{Ca}(\text{OH})_2$ to form ettringite and gypsum, causing expansion and deterioration of concrete strength (Bassuoni and Nehdi 2007, Bondar *et al.* 2015). Brucite ($\text{Mg}(\text{OH})_2$) is also formed due to magnesium sulfate attack and the brucite retards the adverse outcomes of sulfate attack at a preliminary phase. However, in the following stages, decomposition of CSH gel to MSH gel occurs, which results in softening of the binder and decreased mechanical strength (Türker *et al.* 1997). For GPC, alkalis from

geopolymer concrete diffuse into the magnesium sulfate solution, and magnesium and calcium ions diffuse into the subsurface areas to react with the sodium silicate or sodium hydroxide and potassium hydroxides in alkaline solution, resulting in ettringite generation and the poor mechanical performance (Bakharev 2005).

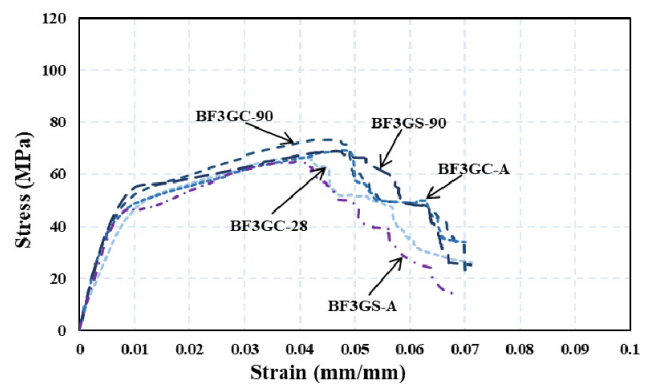
3.2.2 Compressive strength of wrapped specimens

Figs. 8-11 illustrate the stress-strain behavior of geopolymer and ordinary concrete specimens under the ambient and magnesium sulfate environments. Compressive strength of the specimens wrapped with 3- layer of basalt and carbon fabrics increased more than 2 times and 3 times than that of unwrapped specimens, respectively. When the FRP layer decreased to 1-layer, the compressive strength increase was more than 1.5 and 2 times for the basalt and carbon FRP wrapped specimens, respectively. In general, when the fiber in the outermost layer of the fabrics ruptured, the compressive load decreased suddenly and then began to increase again due to the inner layers of the fabrics until the failure of the inner fabrics realized.

Similar to unwrapped specimens, the compressive strength of the wrapped geopolymer specimens under ambient environment increased up to 90 days due to the lower pozzolanic reaction of the fly ash. The compressive strength enhancements of CF3GC-90, BF3GC-90, CF1GC-90, and BF1GC-90 specimens were 8.9%, 10%, 9.3%, and 9.8%, respectively as compared to the 28-day compressive

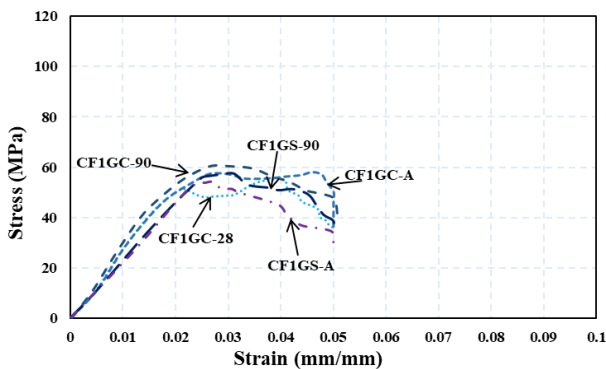


(a) Specimens wrapped with 3-layer of carbon FRP

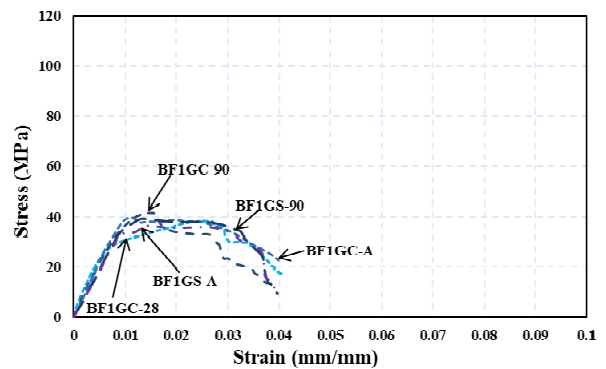


(b) Specimens wrapped with 3-layer of basalt FRP

Fig. 8 Stress-strain behavior of geopolymer specimens wrapped with 3-layer of carbon and basalt FRP

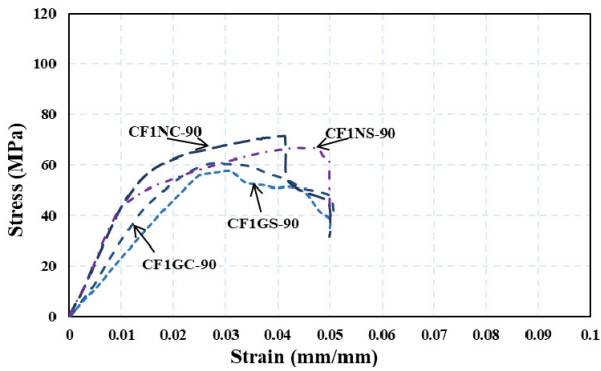


(a) Specimens wrapped with 1-layer of carbon FRP

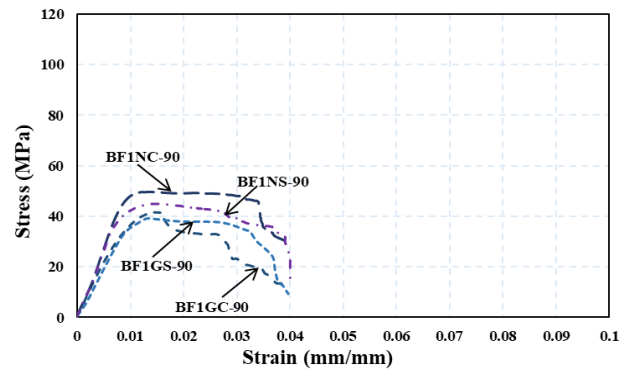


(b) Specimens wrapped with 1-layer of basalt FRP

Fig. 9 Stress-strain behavior of geopolymer specimens wrapped with 1-layer of carbon and basalt FRP



(a) GPC and NC specimens wrapped with 1-layer of carbon FRP



(b) GPC and NC specimens wrapped with 1-layer of basalt FRP

Fig. 10 Stress-strain behavior of GPC and NC specimens wrapped with 1-layer of carbon and basalt FRP

strengths of the CF3GC-28, BF3GC28, CF1GC-28, and BF1GC-28 specimens as shown in Figs. 9 and 10. In the study, the effect of FRP material as a retrofitting material was also investigated. Therefore, the specimens were subjected to 5% magnesium sulfate solutions and then the exposed specimens were wrapped with the carbon and basalt FRP fabrics. The compressive strength improvements of the CF3GC-A, BF3GC-A, CF1GC-A, and BF1GC-A specimens were 4.8%, 4.08%, 4.52%, and 3.82%, respectively as compared to the 28-day compressive strengths of the same specimens. The results showed that the FRP wrappings before the chemical exposure yielded higher compressive strength results than the FRP wrappings after chemical exposure. The amount of compressive strength enhancement increased with an increase in the FRP layer. The specimens under sulfate environment showed poor performance than the specimens under ambient environment. When the compressive strengths of geopolymer concretes were compared to each other, the decrease in the compressive strength of the CF3GS-90, BF3GS-90, CF1GS-90, and BF1GS-90 specimens were 4.2% and 5.8%, 5.9% and 7.8%, respectively than 90-day compressive strength of the CF3GC-90, BF3GC-90, CF1GC-90, and BF1GC-90, respectively. In addition, the compressive strength decrease of the CF3GS-A, BF3GS-A, CF1GS-A, and BF1GS-A specimens were 6.2%, 7.4%, 6.8%, and 8.5% than the 90-day compressive strength of the of the CF3GS-90, BF3GS-90, CF1GS-90, and BF1GS-90

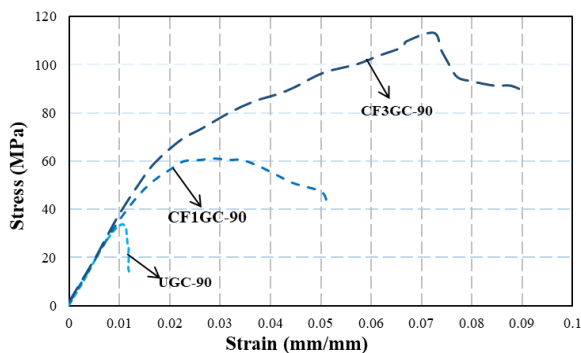
specimens, respectively as shown in Figs. 10 and 11.

When wrapped and unwrapped specimens were compared, at least 25% compressive strength enhancement was observed for the specimens wrapped with 1-layer of basalt FRP fabrics that the least strength enhancement was observed for this type of FRP fabrics. Therefore, it can be concluded that FRP wrappings can be used to strengthening the structural elements subjected to magnesium sulfate environments.

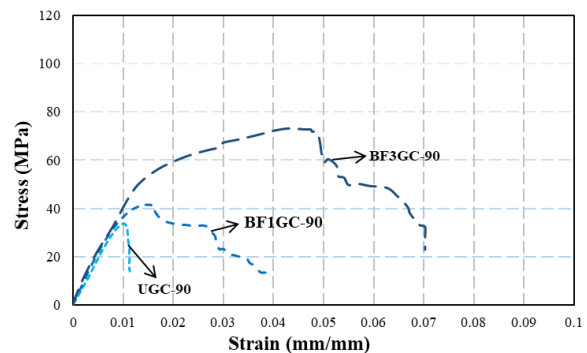
In addition to geopolymer concretes, ordinary concretes were also wrapped with one-layer of FRP fabrics under sulfate attack. The compressive strength reductions of the ordinary concrete specimens due to sulfate attack were found to be 6.84% and 8.63% less than the ordinary specimens under ambient environment. These strength reductions were found to be higher than the strength reductions of GPC specimens, which indicated that the geopolymer concrete specimens showed greater resistance to magnesium sulfate environment than the OPC specimens. In addition, the unwrapped OPC specimens showed 28.47% compressive strength reduction under the sulfate environment. It can be concluded that FRP wrappings provide a good protection to the concrete against chemical attack of magnesium sulfate, and the carbon FRP showed an efficiency higher than basalt FRP.

3.2.3 Ductility response

Fig. 11 illustrates the stress-strain behavior of



(a) Unwrapped GPC and GPC wrapped by CF



(b) Unwrapped GPC and GPC wrapped by BF

Fig. 11 Stress-strain behavior of GPC specimens unwrapped and wrapped with carbon and basalt FRP

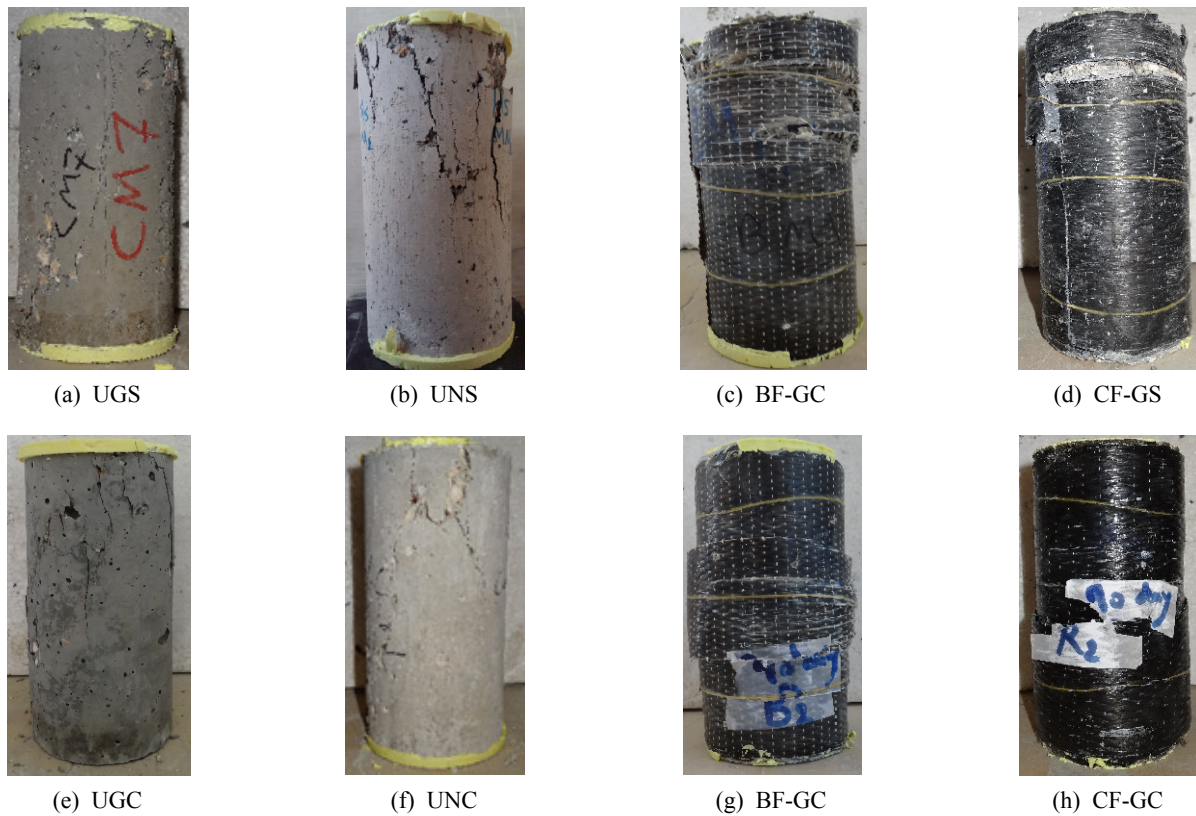


Fig. 12 Failure mode of the specimens exposed to sulfate (a, b, c, d) and ambient (e, f, g, h) environments

geopolymer concretes under ambient environment. The unwrapped geopolymer concrete specimens showed lower ductility than the wrapped specimens. The favourable effect of FRP wrappings on the ductility performance was found obvious. The ductility performance improved with an increase in the wrapping layers of FRP and the highest ductile performance was obtained for the specimens wrapped with 3-layer of carbon FRP fabrics. The improvement in the ductility performance resulted from the increase in both strength and strain capacities due to FRP wrappings. The effect of carbon FRP wrapping on both strength and strain performance of the specimens was found superior than the effect of basalt FRP wrappings. The similar result was also reported in the previous study (Photiou *et al.* 2006).

3.2.4 Failure modes of the specimens under compression load

The expansion of geopolymer concrete occurred during compression loading on the cylinder specimens, and carbon and basalt FRP fabrics resisted the lateral expansion by creating a confinement in the circumferential direction of the cylinder specimens. When tensile stresses due to axial load exceed the FRP fabrics tensile strength resistance, FRP rupture occurred and the failure realized. In addition, the failure due to poor vertical lap joints in FRP fabrics has rarely been reported in the previous studies (Nanni and Bradford 1995, Demers and Neale 1994).

Fig. 12 illustrates the fracture or failure shapes of the specimens under magnesium sulfate and ambient environments. The crack initiation occurred around the top

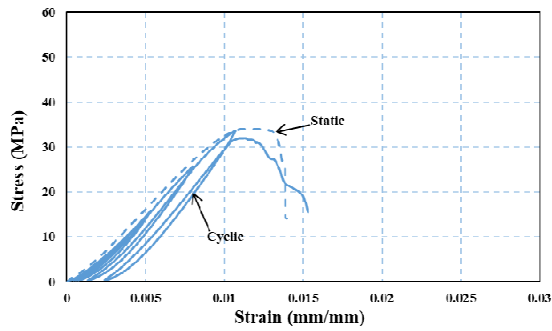
or bottom regions of the specimens and the formed crack openings widened further at these locations until the failure due to high-stress concentrations caused by the friction between the machine plates and the specimen. Since FRP fabrics oriented uni-directional, sudden rupture of the FRP fabrics occurred and hence stress transfer cannot be possible between FRP fibers.

During various stages of tests, small popping noises were heard as stated previous studies (Chaallal *et al.* 2003, Lezgy-Nazargah *et al.* 2018, Taghia and Bakar 2013). It was clearly observed that the failure of the most of the specimens occurred at the top or bottom region of the specimen when the FRP fabrics were taken off upon specimen failure.

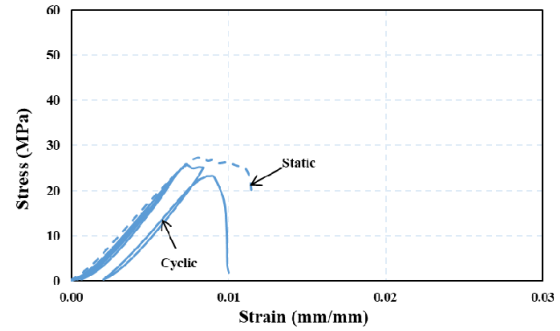
Similar failure modes were observed in both geopolymer and OPC concrete (NC) specimens. However, the failure of the unwrapped specimens occurred more violent than the specimens wrapped with FRP fabrics. The failure of the unwrapped specimens occurred near the top and bottom of the specimens as similar to the wrapped ones as shown in Fig. 12.

3.3 Cyclic loading

Figs. 13 and 14 show the static and cyclic loading behavior of the geopolymer specimens unwrapped and wrapped with one-layer of FRP under magnesium sulfate and ambient environments. The static and cyclic behavior of unwrapped geopolymer specimens showed linear behavior up to the peak load. However, the static and cyclic curve separated from each other for the post-peak curve

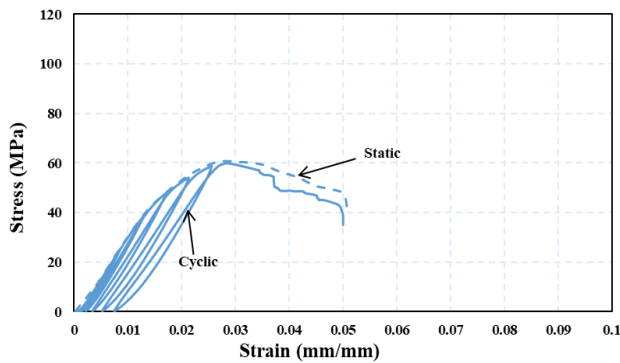


(a) Unwrapped GPC under ambient environment

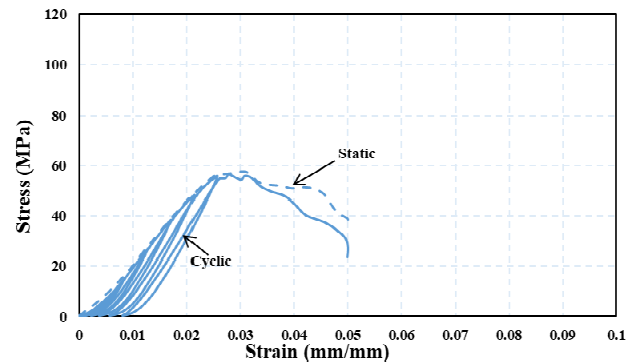


(b) Unwrapped GPC under sulfate environment

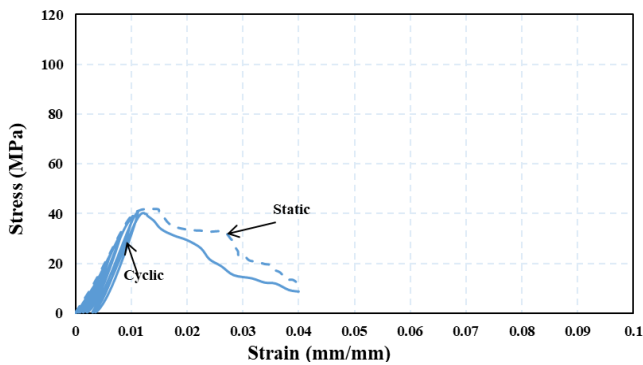
Fig. 13 Behavior of unwrapped geopolymer concrete specimens under static and cyclic loading



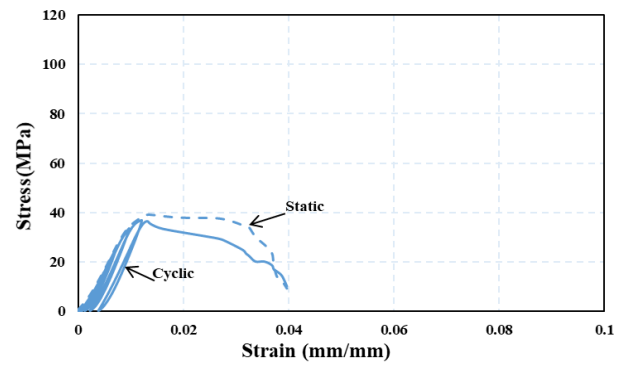
(a) GPC wrapped with 1-layer of carbon FRP under ambient environment



(b) GPC wrapped with 1-layer of carbon FRP under magnesium sulfate environment



(c) GPC wrapped with 1-layer of basalt FRP under ambient environment



(d) GPC wrapped with 1-layer of basalt FRP under magnesium sulfate environment

Fig. 14 Behavior of geopolymer specimens wrapped with carbon and basalt FRP under static and cyclic loading

under magnesium sulfate environment, which may be attributed to the decrease in elastic modulus due to the softening and decreased the rigidity of the specimens with increasing unloading/loading cycles. For the wrapped specimens, similar stress-strain behavior was obtained at both pre-peak curve and post-peak curve for static and cyclic loading under sulfate and ambient environments. The similar behavior under magnesium sulfate environment can be attributed to the elastic behavior of carbon and basalt FRP fabrics, which showed the superior resistance to the cyclic loading. The envelopes of the stress-strain curves of geopolymer specimens under cyclic loading reached by connecting the peaks of the unloading cycles and the obtained curve matched well with the stress-strain curve

under static loading. Similar findings were also found in the previous studies (Lam *et al.* 2006, Shah *et al.* 1983). In addition, the behavior of the specimens wrapped with basalt and carbon FRP fabrics under cyclic loading was found identical (Lam *et al.* 2006 Shah *et al.* 1983).

However, specimens wrapped with carbon FRP fabrics showed higher compressive strength than the specimens wrapped with basalt FRP fabrics as shown in Fig. 14.

3.4 Scanning Electron Microscopy (SEM)

Wrapped and unwrapped geopolymer specimens and unwrapped ordinary concrete (NC) specimens were analyzed in detail by scanning electron microscopy (SEM)

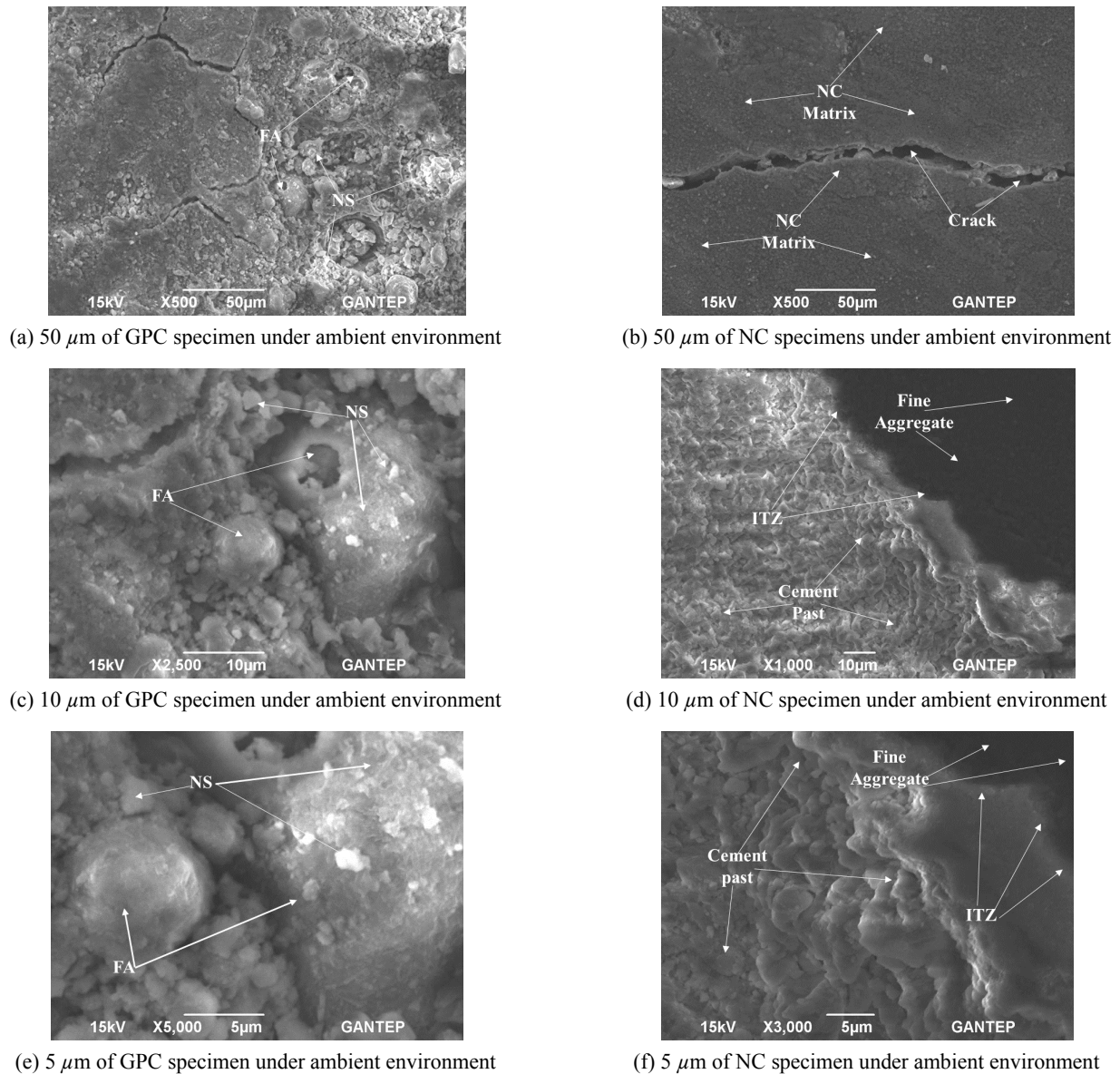


Fig. 15 Different sizes of SEM images of the GPC (a, c, and e) specimens, and NC (ordinary concrete) specimens (b, d, and f) under ambient environment

to observe the changes in the interfacial transition zone (ITZ) between FRP fabrics and matrix under magnesium sulfate attack. In addition, the changes on the surfaces of basalt and carbon FRP fabrics were investigated in microscale. Since the sulfate attack is a surface phenomenon, the deterioration begins at the surface of the concrete and progresses to inside (Attigbe and Rizkalla 1988). Therefore, SEM photos were taken for each specimen from the outermost layer (maximum 1 cm from the outermost layer) of the cylinder specimens as shown in Fig. 4. One inch (2.54 cm) slices of the specimens were cut and discarded from both top and bottom regions and 1 cm thick circular slice from the middle sections of the specimens was used for SEM analysis. Figs. 15 and 16 show the different sizes of the SEM images of the geopolymer (GPC) and OPC concrete (NC) specimens under ambient and magnesium sulfate environments, respectively. The formation of ettringite can cause a color

change, expansion, cracking, spalling and loss of the mechanical performance. The deterioration due to the ettringite formation was found more severe in the ordinary concrete (NC) specimens than the GPC specimens. It can be attributed to the high CaO content in the NC specimens than the fly ash and nano-silica based GPC specimens. The incorporation of the nano-silica particles reduced the porosity and permeability of the specimens due to its denser structure.

Fig. 17 shows the SEM images of the specimens wrapped with carbon and basalt FRP fabrics under magnesium sulfate environment. The influence of the sulfate on the specimens wrapped with FRP was found less than the unwrapped specimens due to the high resistance of carbon and basalt FRP to magnesium sulfate environment. The specimens wrapped with carbon FRP showed less white deposits than the specimens wrapped with basalt FRP. Fig. 18 illustrates the SEM images of the carbon and basalt

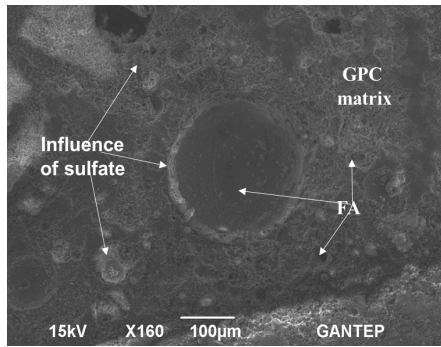
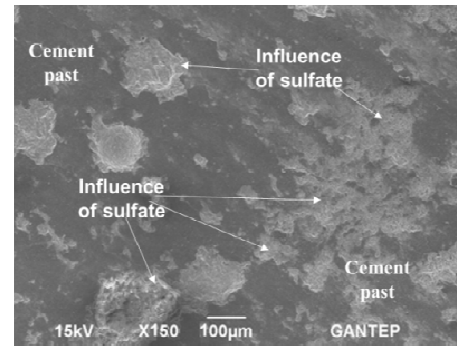
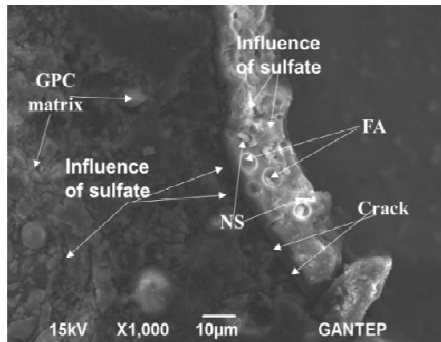
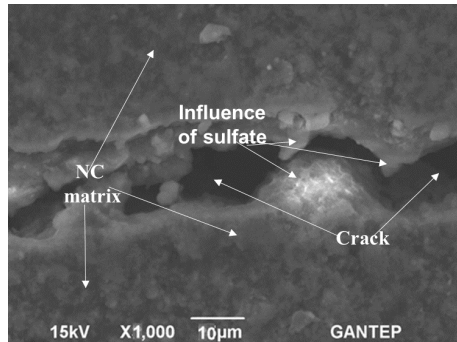
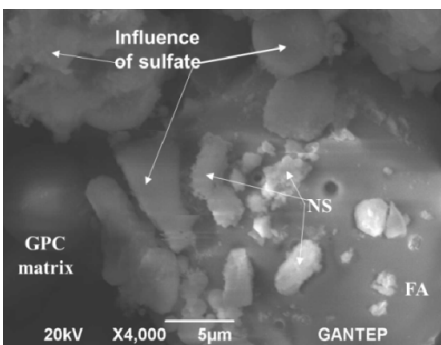
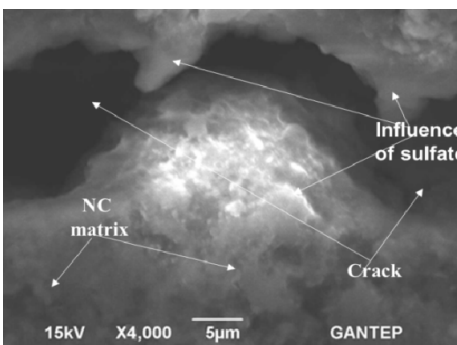
(a) 100 μm of GPC specimen under sulfate environment(b) 100 μm of NC specimen under sulfate environment(c) 10 μm of GPC specimen under sulfate environment(d) 10 μm of NC specimen under sulfate environment(e) 5 μm of GPC specimen under sulfate environment(f) 5 μm of NC specimen under sulfate environment

Fig. 16 Different sizes of SEM images of the GPC (a, c, and e) specimens, and NC (ordinary concrete) specimens (b, d, and f) under magnesium sulfate environment

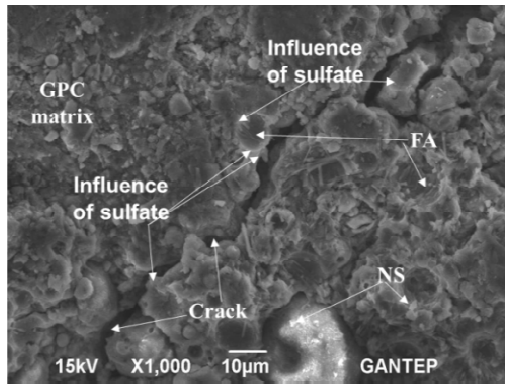
fabrics with and without epoxy. Due to the sensitivity of the epoxy to the sulfate environment, carbon and basalt FRP fabrics were also significantly affected by the magnesium sulfate attack. In addition, carbon FRP fabrics were less affected than the basalt FRP fabrics due to the higher bond between carbon FRP fabrics and the epoxy.

4. Conclusions

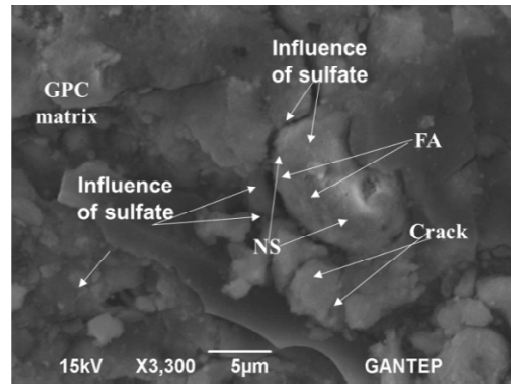
In this study, the effects of magnesium sulfate solution on the mechanical performance and durability properties of the confined and unconfined specimens were investigated in detail. Carbon and basalt FRP fabrics with different layers were used and another reason for the use of FRP materials in GPC specimens was to decrease the degradation effect of magnesium sulfate attack. A comprehensive experimental study was carried out using static and cyclic loading tests to

achieve the aims of the study. In addition, SEM observation were also conducted to observe the changes on the surface of carbon and basalt FRP fabrics and the interfacial transition zone between matrix and FRP fabrics. General findings were summarized as follows:

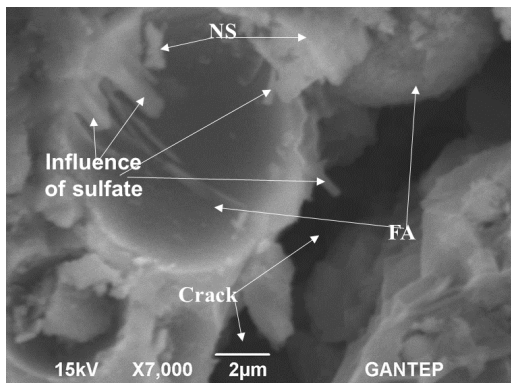
- Visual inspection results indicated that all specimens maintained their initial conditions without cracking and spalling after two-month exposure to magnesium sulfate environment. However, FRP fabrics slightly affected by the sulfate and the highest color change occurred in the basalt FRP fabrics than the carbon FRP fabrics.
- Weight change results in the ambient environment showed that the weight loss was observed for all specimens due to continuous hydration reactions. The weight loss of OPC specimens was found 3-times higher than the weight loss of GPC specimens



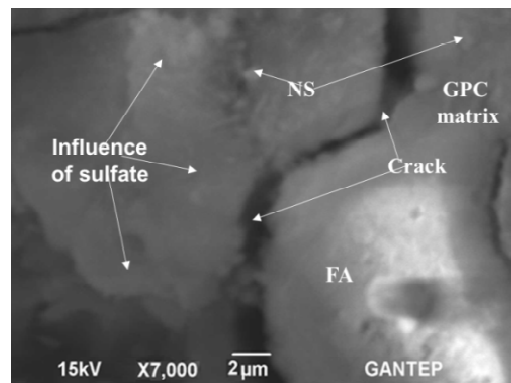
(a) 10 μm of CFGPC specimen under sulfate environment



(b) 10 μm of BFGPC specimen under sulfate environment

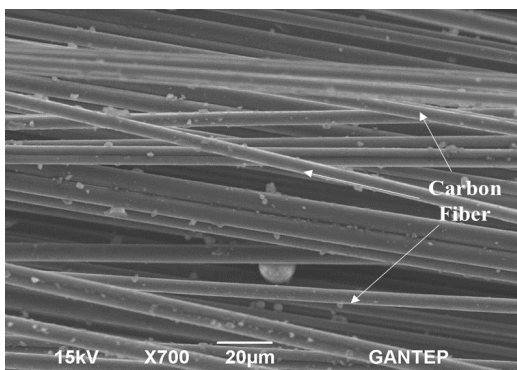


(c) 2 μm of CFGPC specimen under sulfate environment

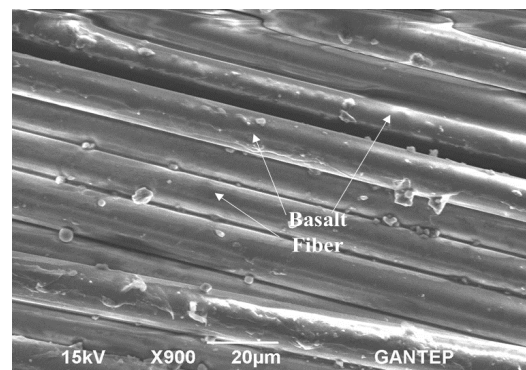


(d) 2 μm of BFGPC specimen under sulfate environment

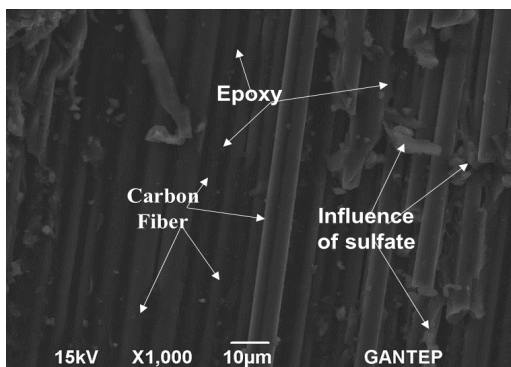
Fig. 17 Different sizes of SEM images of the geopolymer specimens wrapped with carbon (a and c) and basalt FRP fabrics (b and d) under magnesium sulfate environment



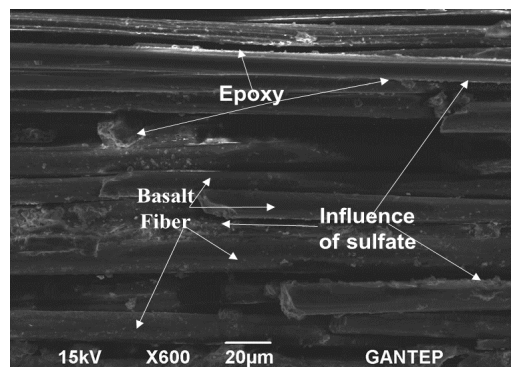
(a) 20 μm CFGPC specimen (w/o epoxy) under ambient env.



(b) 20 μm BFGPC specimen (w/o epoxy) under ambient env.



(c) 20 μm of CFGPC specimen (with epoxy) under sulfate env.



(d) 20 μm of BFGPC specimen (with epoxy) under sulfate env.

Fig. 18 SEM images of the carbon and basalt FRP fabric sheets

due to the completion of hydration reactions for GPC specimens on the first days. In addition, similar weight loss was observed for the all specimens wrapped with FRP fabrics.

- Weight change results in the magnesium sulfate environment indicated that the weight gain was observed for all specimens, except for unwrapped ordinary concrete specimens. The highest weight increase occurred on unwrapped GPC specimens. In addition, specimens wrapped with FRP showed less weight gain and the specimens with 3-layer FRP wrappings showed the better sulfate resistance than the specimens with 1-layer of FRP wrapping and unwrapped specimens, respectively. The carbon FRP wrapped specimens showed the superior sulfate resistance than the basalt FRP wrapped specimens.
- Stress-strain behavior of the specimens illustrated that GPC specimens showed lower compressive strength and strain values than ordinary concrete specimens. It may be attributed to the low activity of fly ash, low CaO content and unreacted nano-silica particles in the GPC specimens. However, GPC specimens showed better resistance to magnesium sulfate environment than ordinary concrete specimens due to the denser structure resulted from the nano-silica particles and the low CaO content that responsible for the deterioration of concrete under chemical attacks.
- The incorporation of FRP fabrics into the geopolymer and ordinary concrete specimens enhanced compressive strength and ductility significantly. These properties further improved as the number of FRP layers increased from 1-layer to 3-layer. In addition, specimens wrapped with carbon FRP showed better mechanical performance and durability than specimens wrapped with basalt FRP in both sulfate and ambient environments. The poor performance was obtained in the unwrapped specimens.
- Specimens wrapped with FRP after the 90-day magnesium sulfate attack indicated that carbon and basalt FRP materials can be used as a rehabilitation material in the magnesium sulfate environment.
- The connection of the envelopes of the axial stress-strain curve of specimens showed similar behavior under static and cyclic loading. The static and cyclic curves of the unwrapped geopolymer specimens showed linear behavior at the pre-peak region in both ambient and magnesium sulfate environments. However, the curves separated from each other in the post-peak region under magnesium sulfate environment. It can be attributed to the decrease in elastic modulus due to the softening and the decreased rigidity of the specimens with increasing unloading/loading cycles. In addition, similar stress-strain behavior was obtained in both pre-peak and post-peak regions for the FRP wrapped specimens, which showed greater resistance against cyclic loading in the ambient and magnesium sulfate environments due to the elastic behavior of carbon and basalt FRP fabrics.

- SEM results showed that geopolymer specimens were found more durable than ordinary concrete specimens under magnesium sulfate attack. It can be attributed to the low CaO content and the existence of nano-silica material that decreased the porosity and permeability of specimens due to its denser structure. In addition, specimens wrapped with carbon and basalt FRP showed greater durability properties (reduced amount of white deposits) than unconfined specimens due to the high resistance of carbon and basalt FRP fabrics to the magnesium sulfate environment. The superior resistance was obtained in specimens wrapped with carbon FRP fabrics.
- Due to the sensitivity of the epoxy to the sulfate environment, carbon and basalt FRP fabrics were also influenced by the magnesium sulfate environment. Due to the high bond between epoxy and carbon FRP fabrics, carbon FRP fabrics were less affected than the basalt FRP fabrics.

References

- Abdelrahman, K. and El-Hacha, R. (2011), "Behavior of large-scale concrete columns wrapped with CFRP and SFRP sheets", *J. Compos. Constr.*, **16**(4), 430-439.
- ASTM C267 (2003), Standard Test Methods For Chemical Resistance Of Mortars, Grouts, And Monolithic Surfacing And Polymer Concretes; American Society for Testing and Materials, West Conshohocken, PA, USA.
- ASTM C39/C39M-12 (2012), Standard Test Method For Compressive Strength Of Cylindrical Concrete Specimens; Annual book of ASTM standard, (Vol. 4-2), Philadelphia, PA, USA.
- Attiogbe, E.K. and Rizkalla, S.H. (1988), "Response of concrete to sulfuric acid attack", *ACI Mater. J.*, **85**(6), 481-488.
- Bakharev, T. (2005), "Resistance of geopolymer materials to acid attack", *Cement Concrete Res.*, **35**(4), 658-670.
- Bakis, C.E., Bank, L.C., Brown, V.L., Cosenza, E., Davalos, J.F., Lesko, J.J., Machida, A., Rizkalla, S.H. and Triantafillou, T.C. (2002), "Fiber-reinforced polymer composites for construction — State-of-the-art review", *J. Compos. Constr.*, **6**(2), 73-87.
- Baldvin, E. (2011), "Experimental Research on BFRP Confined Concrete Columns", Master of Science Thesis; University of Reykjavik, Iceland.
- Bassuoni, M.T. and Nehdi, M.L. (2007), "Resistance of self-consolidating concrete to sulfuric acid attack with consecutive pH reduction", *Cement Concrete Res.*, **37**(7), 1070-1084.
- Belkowitz, J.S., Belkowitz, W.L.B., Nawrocki, K. and Fisher, F.T. (2015), "Impact of nanosilica size and surface area on concrete properties", *ACI Mater. J.*, **112**(3), 419-427. DOI: <https://doi.org/10.14359/51687397>
- Bondar, D., Lynsdale, C.J., Milestone, N.B. and Hassani, N. (2015), "Sulfate Resistance of Alkali Activated Pozzolans", *Int. J. Concrete Struct. Mater.*, **9**(2), 145-158.
- Chaallal, O., Hassan, M. and Shahawy, M. (2003), "Confinement model for axially loaded short rectangular columns strengthened with fiber-reinforced polymer wrapping", *Struct. J.*, **100**(2), 215-221.
- Çevik, A., Alzebaree, R., Humur, G., Niş, A. and Gülşan, M.E. (2018), "Effect of nano-silica on the chemical durability and mechanical performance of fly ash based geopolymer concrete", *Ceramics Int.*, **44**(11), 12253-12264.
- Chi, M. and Huang, R. (2013), "Binding mechanism and

- properties of alkali-activated fly ash/slag mortars”, *Constr. Build. Mater.*, **40**, 291-298.
- Chindaprasirt, P., Rattanasak, U. and Taebuanhuad, S. (2012), “Resistance to acid and sulfate solutions of microwave-assisted high calcium fly ash geopolymer”, *Mater. Struct.*, **46**(3), 375-381.
- Davidovits, J. (1994), “Properties of geopolymer cements”, *Proceedings of the First International Conference on Alkaline Cements and Concretes*, Kiev State Technical University, Ukraine: Scientific Research Institute on Binders and Materials, **1**, 131-149.
- Deb, P.S., Nath, P. and Sarker, P.K. (2014), “The effects of ground granulated blast-furnace slag blending with fly ash and activator content on the workability and strength properties of geopolymer concrete cured at ambient temperature”, *Mater. Des.*, **62**, 32-39.
- Demers, M. and Neale, K.W. (1994), “Strengthening of concrete columns with unidirectional composite sheets”, *Development in Short and Medium Span Bridge Engineering '94, Proceedings, 4th International Conference on Short and Medium Bridges*, (A.A. Mufti, B. Bakht, and L.G. Jaeger, Eds.), Canadian Society for Civil Engineering, Montreal, Canada, pp. 895-905.
- Dombrowski, K., Buchwald, A. and Weil, M. (2007), “The influence of calcium content on the structure and thermal performance of fly ash based geopolymers”, *J. Mater. Sci.*, **42**(9), 3033-3043.
- Duxson, P., Fernández-Jiménez, A., Provis, J.L., Lukey, G.C., Palomo, A. and Van Deventer, J.S.J. (2007), “Geopolymer technology: the current state of the art”, *J. Mater. Sci.*, **42**(9), 2917-2933.
- Garg, D.M., Sharma, S., Sharma, S. and Mehta, R. (2017), “Effect of hygrothermal aging on GFRP composites in marine environment”, *Steel Compos. Struct., Int. J.*, **25**(1), 93-104.
- Gülşan, M.E., Mohammedameen, A., Şahmaran, M., Niş, A., Alzebaree, R. and Çevik, A. (2018), “Effects of sulphuric acid on mechanical and durability properties of PVA-ECC composites confined with CFRP and BFRP fabrics”, *Adv. Concrete Constr., Int. J.*, **6**(2), 199-220.
- Hamilton, H.R., Benmokrane, B., Dolan, C.W. and Sprinkel, M.M. (2009), “Polymer materials to enhance performance of concrete in civil infrastructure”, *Polym. Rev.*, **49**(1), 1-24.
- Hardjito, D. and Rangan, B.V. (2005), “Development and properties of low-calcium fly ash-based geopolymer concrete”, Research Report GC 1; Faculty of Engineering Curtin University of Technology Perth, Australia.
- Hardjito, D., Wallah, S.E., Sumajouw, D.M.J. and Rangan, B.V. (2004), “On the development of fly ash-based geopolymer concrete”, *Mater. J.*, **101**(6), 467-472.
- Jo, B.W., Park, S.K. and Park, M.S. (2007), “Strength and hardening characteristics of activated fly ash mortars”, *Magaz. Concrete Res.*, **59**(2), 121-129.
- Khale, D. and Chaudhary, R. (2007), “Mechanism of geopolymerization and factors influencing its development: A review”, *J. Mater. Sci.*, **42**(3), 729-746.
DOI: <https://doi.org/10.1007/s10853-006-0401-4>
- Kumaravel, S. and Girija, K. (2013), “Acid and salt resistance of geopolymer concrete with varying concentration of NaOH”, *J. Eng. Res. Studies*, **4**(4), 1-3.
- Lam, L., Teng, J.G., Cheung, C.H. and Xiao, Y. (2006), “FRP-confined concrete under axial cyclic compression”, *Cement Concrete Compos.*, **28**(10), 949-958.
- Lezgy-Nazargah, M., Dezhangah, M. and Sephrinia, M. (2018), “The effects of different FRP/concrete bond-slip laws on the 3D nonlinear FE modeling of retrofitted RC beams — A sensitivity analysis”, *Steel Compos. Struct., Int. J.*, **26**(3), 347-360.
- Li, Z. and Ding, Z. (2003), “Property improvement of Portland cement by incorporating with metakaolin and slag”, *Cement Concrete Res.*, **33**(4), 579-584.
- Li, S. and Roy, D.M. (1988), “Preparation and characterization of high and low CaO/SiO₂ ratio “pure” C--S--H for chemically bonded ceramics”, *J. Mater. Res.*, **3**(2), 380-386.
- Liu, H., Zhang, Q., Li, V., Su, H. and Gu, C. (2017), “Durability study on engineered cementitious composites (ECC) under sulfate and chloride environment”, *Constr. Build. Mater.*, **133**, 171-181.
- Lloyd, N. and Rangan, B.V. (2010), “Geopolymer Concrete: a Review of Development and Opportunities”, *Proceedings of the 35th Conference on Our World in Concrete & Structures*.
- Lokuge, W., Setunge, S. and Sanjayan, J.G. (2010), “Stress-strain model for high strength concrete confined by FRP”, *Proceedings of the 21st Australasian Conference on the Mechanics of Structures and Materials: Incorporating Sustainable Practice in Mechanics of Structures and Materials (ACMSM21)*, pp/ 481-486.
- Mobili, A., Belli, A., Giosuè, C., Bellezze, T. and Tittarelli, F. (2016), “Metakaolin and fly ash alkali-activated mortars compared with cementitious mortars at the same strength class”, *Cement Concrete Res.*, **88**, 198-210.
- Nanni, N. and Bradford, N.M. (1995), “FRP jacketed concrete under uniaxial compression”, *Constr. Build. Mater.*, **9**(2), 115-124.
- Nazari, A. and Sanjayan, J.G. (2015), “Modelling of compressive strength of geopolymer paste, mortar and concrete by optimized support vector machine”, *Ceramics Int.*, **41**(9), 12164-12177.
- Olivia, M. and Nikraz, H. (2012), “Properties of fly ash geopolymer concrete designed by Taguchi method”, *Mater. Des. (1980-2015)*, **36**, 191-198.
- Partha, S.D., Pradip, N. and Prabir, K.S. (2013), “Strength and permeation properties of slag blended fly ash based geopolymer concrete”, *Adv. Mater. Res.*, **651**, 168-173.
- Photiou, N.K., Hollaway, L.C. and Chryssanthopoulos, M.K. (2006), “Strengthening of an artificially degraded steel beam utilising a carbon / glass composite system”, In: *Advanced Polymer Composites for Structural Applications in Construction*, **20**, 11-21.
DOI: <https://doi.org/10.1016/j.conbuildmat.2005.06.043>
- Shah, S.P., Fafitis, A. and Arnold, R. (1983), “Cyclic loading of spirally reinforced concrete”, *J. Struct. Eng.*, **109**(7), 1695-1710.
- Soroka, I. (1979), *Portland Cement Paste and Concrete*, Macmillan Press, London, UK, pp. 151-152.
- Taghia, P. and Bakar, S.A. (2013), “Mechanical behaviour of confined reinforced concrete-CFRP short column-based on finite element analysis”, *World Appl. Sci. J.*, **24**(7), 960-970.
- Taylor, H.F.W., Famy, C. and Scrivener, K.L. (2001), “Delayed ettringite formation”, *Cement Concrete Res.*, **31**(5), 683-693.
- Thokchom, S., Ghosh, P. and Ghosh, S. (2010), “Performance of fly ash based geopolymer mortars in sulphate solution”, *J. Eng. Sci. Technol. Rev.*, **3**(1), 36-40.
- Tulliani, J., Montanaro, L., Negro, A. and Collepardi, M. (2002), “Sulfate attack of concrete building foundations induced by sewage waters”, *Cement Concrete Res.*, **32**(6), 843-849.
- Türker, F., Aköz, F., Koral, S. and Yüzer, N. (1997), “Effects of magnesium sulfate concentration on the sulfate resistance of mortars with and without silica fume”, *Cement Concrete Res.*, **27**(2), 205-214.
- Visitanupong, C. (2009), “Durability of Fly ash Based Geopolymer Mortar”, Thesis Approval; Graduate School, Kasetsart University, Thailand.
- Wallah, S.E. and Rangan, B.V. (2006), “Low-Calcium Fly Ash-Based Geopolymer Concrete: Long-Term Properties”, Curtin Research Publication Report.
- Wallah, S.E., Hardjito, D., Sumajouw, D.M.J. and Rangan, B.V. (2005), “Sulfate and acid resistance of fly ash-based

geopolymer concrete”, *Proceedings of the Australian Structural Engineering Conference Sydney, N.S.W.: Engineers Australia*, pp. 733-742.

Wang, P., Jiang, M., Chen, H., Jin, F., Zhou, J., Zheng, Q. and Fan, H. (2017), “Load carrying capacity of CFRP retrofitted broken concrete arch”, *Steel Compos. Struct., Int. J.*, **23**(2), 187-194.

Zhang, Z. and Zhang, Q. (2017), “Self-healing ability of Engineered Cementitious Composites (ECC) under different exposure environments”, *Constr. Build. Mater.*, **156**, 142-151.

CC